NASA MEMO 10-18-58L



# NASA

# MEMORANDUM

## EFFECT OF TARGET THICKNESS ON CRATERING AND PENETRATION OF PROJECTILES IMPACTING AT VELOCITIES TO 13,000 FEET PER SECOND

By William H. Kinard, C. H. Lambert, Jr., David R. Schryer, and Francis W. Casey, Jr.

Langley Research Center
Langley Field, Va.

NATIONAL AERONAUTICS AND SPACE ADMINISTRATION
WASHINGTON
December 1958
Declassified April 12, 1961

NATIONAL AERONAUTICS AND SPACE ADMINISTRATION

MEMORANDUM 10-18-58L

# EFFECT OF TARGET THICKNESS ON CRATERING AND PENETRATION OF PROJECTILES IMPACTING AT VELOCITIES TO 13,000 FEET PER SECOND*

By William H. Kinard, C. H. Lambert, Jr., David R. Schryer, and Francis W. Casey, Jr.

## SUMMARY

In order to determine the effects of target thickness on the penetration and cratering of a target resulting from impacts by high-velocity projectiles, a series of experimental tests have been run. The projectile-target material combinations investigated were aluminum projectiles impacting aluminum targets and steel projectiles impacting aluminum and copper targets. The velocity spectrum ranged from 4,000 ft/sec to 13,000 ft/sec. It has been found that the penetration is a function of target thickness provided that the penetration is greater than 20 percent of the target thickness. Targets of a thickness such that the penetration amounts to less than 20 percent of the thickness may be regarded as quasi-infinite. An empirical formula has been established relating the penetration to the target thickness and to the penetration of a projectile of the same mass, configuration, and velocity into a quasi-infinite target. In particular, it has been found that a projectile can completely penetrate a target whose thickness is approximately one and one-half times as great as the penetration of a similar projectile into a quasi-infinite target. The diameter of a crater has also been found to be a function of the target thickness provided that the target thickness is not greater than the projectile length in the case of cylindrical projectiles and not greater than two to three times the projectile diameter in the case of spherical projectiles.

## INTRODUCTION

With the advent of intercontinental ballistic missiles and satellite vehicles, which while traveling above the earth's atmosphere may possibly encounter meteoric particles, much interest has been aroused in the

*Title, Unclassified.

phenomena of ultra-high-speed impacts. Space vehicles may encounter particles ranging from a few mils to an inch or greater and the impact velocity may be as great as 250,000 feet per second.

Designers of space vehicles must have some means of estimating the depth a particle can penetrate in order to determine the skin thickness necessary to defeat the particle and to protect the personnel or instrumentation inside the vehicle. Several investigations (for example, refs. 1 and 2) have been conducted to determine the penetration of projectiles impacting quasi-infinite metal targets and various empirical formulas have been suggested for predicting such penetration. Space vehicles, however, will be designed to have skins as thin as possible. Therefore, this study was made to investigate the effects of target thickness on penetration and cratering within the velocity range presently obtainable in the laboratory.

## SYMBOLS

| | |
|---|---|
| $P$ | penetration, in. |
| $P_\infty$ | penetration in a quasi-infinite target, in. |
| $t_T$ | target thickness, in. |
| $T_a$ | aluminum target |
| $T_c$ | copper target |
| $S_s$ | steel projectile |
| $S_a$ | aluminum projectile |
| $L$ | projectile length, in. |
| $d_S$ | projectile diameter, in. |
| $V$ | projectile velocity, ft/sec |
| $d_C$ | crater diameter |
| $c$ | speed of sound in target material, ft/sec |

$\rho_T$ density of target material, lb/in.$^3$

$\rho_S$ density of projectile material, lb/in.$^3$

## APPARATUS AND TEST TECHNIQUE

### Gun Facilities

Photographs of the gun installations used to accelerate the projectiles are shown in figures 1, 2, and 3.

Figure 1 shows the standard 220 Swift rifle that was used to fire projectiles of 0.22-inch diameter and smaller at velocities of 6,400 ft/sec and below. Standard 220 Swift cartridges were used with varying quantity of Hercules Unique rifle powder to produce the desired velocities.

Figure 2 shows the helium gun which was used to propel projectiles in this investigation to a velocity of 13,000 ft/sec. The helium gun consists of a 20-millimeter pump tube and a 22-caliber launch tube. The helium is compressed by a shock wave formed by the burning powder charge and provides the force to launch the projectile.

For the firings in this investigation, a helium pressure of 900 lb/sq in. and a powder charge of 250 grains of Hercules Unique rifle powder was used in the pump tube. The launch tube and vacuum chamber were evacuated to a pressure of 1 millimeter of mercury.

Figure 3 shows the arrangement for the 50-caliber experimental proof gun. Hercules Unique rifle powder was used to accelerate the projectiles which traveled at a velocity of 5,900 ft/sec.

### Projectiles and Sabots

Spheres of two diameters, 1/16 inch and 1/2 inch, were fired. Both the 220 Swift rifle and the helium gun were used to fire $\frac{1}{16}$-inch spheres, and the 50-caliber gun was used to fire $\frac{1}{2}$-inch spheres.

Since the $\frac{1}{16}$-inch spheres had a diameter smaller than the bore of the barrels from which they were fired, sabots had to be used.

Consequently, a method was needed to prevent the impact craters caused by the spheres from being altered by the impact of the sabots.

The method employed was to deflect the sabots by causing them to strike the edge of a steel deflector plate, placed so that the edge of the plate protruded slightly above the lip of the gun barrel but remained below the flight path of the projectiles.

No sabots were needed for firing $\frac{1}{2}$-inch spheres from the 50-caliber gun.

All cylinders fired were 0.22 inch in diameter and were fired without sabots from the 220 Swift rifle.

## Instrumentation

The usefulness of each of the various systems for measuring velocities is dependent upon many factors including the velocities to be measured and many physical aspects of the installation with which the system is to be associated. In this study it was found to be advantageous to use a somewhat different velocity measuring system with each gun.

For the 220 Swift rifle, velocities were measured by the breaking of two painted circuits placed a known distance apart in the flight path of the projectile as shown in figure 1. The time interval between the breaking of the two circuits was measured with a Hewlett-Packard precision electronic counter with a time interval unit. All quoted velocities have been corrected for drag between the center of the measured distance and the target.

For the velocity determinations on a helium gun, two 0.001-inch-thick sheets of aluminum foil were placed in the vacuum tank in the flight path of the projectile so that they were visible from the outside through the tank side windows. As the sphere impacted each foil sheet a blip of light was generated. By recording these blips on a high-speed drum camera with the film moving in the plane perpendicular to the flight of the sphere, the velocity could be determined from the angle between the blips. One sphere was recovered after impacting the aluminum foil by allowing it to penetrate into Styrofoam. No damage could be observed on the sphere, indicating that the foil did not harm it.

The velocities of the $\frac{1}{2}$-inch-diameter spheres fired from the 50-caliber gun were measured by using two condenser microphones placed adjacent to the flight path of the sphere. The time necessary for the

projectile to traverse the known distance between the microphones was measured with a Hewlett-Packard precision electronic counter with a time interval unit.

Figure 3 also shows the high-framing-rate, argon-flash photography arrangement used for impact pictures in this study. A detailed description of the arrangement is given in reference 3. The system consists of (1) a specially designed explosive-train system to give the desired time delay between luminous shocks produced in argon, (2) a plastic Fresnel condensing lens, and (3) three still cameras.

One group of copper targets was prepared for metallurgical examination. Models were cut by a water-cooled specimen cutter. The sections were taken parallel and perpendicular to the direction of impact. The surface was prepared by using standard metallographic polishing techniques with varying concentrations (0 to 30 percent) of nitric acid for etching. Photographs were taken by using a photomicroscope with a magnification of ×120.

## RESULTS AND DISCUSSION

### Effect of Target Thickness on Crater Diameter

Figure 4 shows two graphs of crater diameter divided by projectile diameter plotted against target thickness divided by projectile length. Figure 4(a) shows the measured crater diameters obtained with $\frac{1}{16}$-inch- and $\frac{1}{2}$-inch-diameter spheres of aluminum impacting aluminum targets at velocities from 5,900 to 13,000 ft/sec and $\frac{1}{16}$-inch-diameter steel spheres impacting copper targets at a velocity of 6,300 ft/sec. Figure 4(b) shows measured crater diameters produced by 0.22-inch-diameter aluminum cylinders having length-to-diameter ratios of 1/2 and 1 impacting aluminum targets at velocities from 4,500 to 6,300 ft/sec.

Results obtained with both spheres and cylinders show that, as the thickness of the target plate approaches zero, the diameter of the crater or hole formed approaches the diameter of the impacting projectile. In the case of spherical projectiles, the crater diameter reaches a maximum value when the target thickness is between two and three times the projectile length (or diameter) and all other factors are held constant. The crater diameters of impacting cylinders reach a maximum when the target thickness is approximately equal to the projectile length. Increasing the thickness of the target more than the projectile length in the case

of cylindrical projectiles and three times the projectile length in the case of spheres apparently has no effect on the diameter of the craters formed.

A metallurgical examination of the target material at the sides of the crater and adjacent to the target surface revealed that the thickness of the layer of deformed crystals which had undergone plastic flow increased along with the crater diameter when the target thickness was increased.

## Effect of Target Thickness on Penetration

A series of aluminum and copper target plates were impacted by spherical and cylindrical projectiles which penetrated from 7 to very nearly 100 percent of the target thickness. Impacts which resulted in complete penetration of the target are not included because in such cases it was not known whether or not the penetrating projectile possessed any residual momentum after achieving the penetration.

The measured penetrations obtained in these tests are presented in figure 5. This figure shows that penetration is independent of target thickness provided that the penetration amounts to less than 20 percent of the target thickness. Thus, a target which is penetrated to a depth which is less than 20 percent of its thickness may be regarded as quasi-infinite. For impacts involving targets which are not quasi-infinite, the penetration increases with decreasing target thickness under otherwise identical impact conditions.

In an effort to establish a physical picture of the conditions that allow the penetration to increase as the ratio of penetration to target thickness increases, several copper targets of varying thickness which had been impacted under the same conditions were cross-sectioned and examined under a metallurgical microscope. The examination of the targets for which the penetration was less than 20 percent of the target thickness showed a relatively thin layer of material directly beneath the crater which had undergone plastic flow. The remainder of the target material between this layer and the back surface of the target showed no evidence of the grain structure having been disturbed. In targets having a crater depth nearly 20 percent of the target thickness it was discovered that, in addition to the layer of deformed material directly beneath the crater, a second layer of material near the back surface had been deformed and small fractures could be observed. As crater depth became a progressively larger percentage of target thickness, a progressively greater deformation of the target crystal structure was observed. When a crater depth of roughly 60 percent of target thickness was reached plastic flow was evident in the entire region between the crater bottom and the back surface of the target.

These observations may give some evidence as to why projectiles penetrate deeper into thinner targets than quasi-infinite targets. In particular, the observation that, when the crater depth is between 20 percent and roughly 60 percent of the target thickness, plastic flow occurs directly beneath the crater and also in a region adjacent to the back surface of the target with an undisturbed region in between indicates that possibly some form of the reflected wave theory, which has been used to explain the scabbing of the back surface of metal plates held in contact with high explosives (ref. 4) may also apply to impact studies.

The reflected wave theory as it would apply to impact studies states that an elastic compression wave is generated when a metal target is suddenly subjected to a very high impulse load. This elastic compression wave travels through the target and is reflected from its back surface as a tension wave. It appears that this reflected wave, or some combination of the reflected wave and the remainder of the oncoming compression wave, may alter the condition of the target material in such a way as to decrease its resistance to penetration. The exact mechanism by which this is brought about is not clearly understood. However, no matter what the mechanism is, it is reasonable that the effect on the penetration would be dependent upon the strength and relative position of the reflected wave during the penetration process. Since both of these factors depend upon the target thickness, the degree of penetration would also be expected to depend upon the target thickness, except in the case of a quasi-infinite target for which the attenuation and/or delay of the wave would be great enough to render it ineffective.

Figure 6 shows three microphotographs of three areas between the bottom of a cross-sectioned crater and the target back surface. Figure 6(a) shows the material adjacent to the crater bottom which has undergone plastic flow. Figure 6(b) shows the undisturbed material between the crater bottom and the back surface. Figure 6(c) shows the deformation and fractures near the target back surface. The depth of the crater in this target is approximately 30 percent of the target thickness.

Figure 7 shows a shadowgraph of an aluminum target being impacted by a steel sphere. The bulge can be seen forming on the back surface along with a shock wave established in the air by the forming of the bulge. The $\frac{1}{2}$-inch-diameter steel sphere in this case penetrated approximately 60 percent of the 1-inch-thick target.

The data from figure 5 were replotted in figure 8 with gain in penetration divided by the penetration achieved in a quasi-infinite target plotted against the percent of the target thickness penetrated.

It can be noted that little gain in penetration is apparent until the depth of penetration becomes approximately 20 percent of the target thickness. As the percent of the target thickness increases above 20 percent, the value of the gain in penetration due to target thickness increases until it becomes 50 percent above the penetration in a quasi-infinite target when the penetration is exactly equal to the target thickness. The line which could be very nearly faired through the data points was found to have the equation

$$\frac{P}{t_T} = 1.3\sqrt{\frac{P - P_\infty}{P_\infty}} \tag{1}$$

The random scatter of the data points about this line is small considering the normal variation found in penetration data.

Solving equation (1) for $P$ gives

$$P = \frac{P_\infty}{\frac{1}{2}\left[1 + \sqrt{1 - 2.367\left(\frac{P_\infty}{t_T}\right)^2}\right]} \tag{2}$$

With the use of equation (2) it is possible to approximate the actual penetration in a certain thickness target when the penetration in a quasi-infinite target under the same conditions is known.

For the case of steel spheres impacting copper targets in the velocity range of 4,000 to 11,500 ft/sec, the penetration in quasi-infinite targets can be predicted by the equation

$$\frac{P_\infty}{d_S} = 2.18\left(\frac{V}{c}\right)\left(\frac{\rho_S}{\rho_T}\right) \tag{3}$$

given in reference 2. By substituting equation (3) for $P_\infty$ into equation (2), the following equation can be obtained to approximate the penetration of steel spheres into copper targets of any thickness:

$$P = \frac{d_S \frac{V}{c} \frac{\rho_S}{P_T}}{\frac{1}{2}\left[1 + \sqrt{1 - 2.367\left(\frac{d_S \frac{V}{c} \frac{\rho_S}{\rho_T}}{t_T}\right)^2}\right]} \tag{4}$$

In order to determine the thickness of a copper target that can be completely penetrated by a sphere, equation (4) can be simplified since the penetration is equal to target thickness and the following equation is obtained for this thickness:

$$t_T = 3.47\left(\frac{V}{c}\right)\left(\frac{\rho_S}{\rho_T}\right)\left(d_S\right) \tag{5}$$

It should be mentioned that equation (5) is slightly optimistic in that a projectile must penetrate a distance slightly more than the thickness of a target to completely penetrate it because of the phenomenon of bulging on the back surface.

Figure 9 shows a group of high-speed shadowgraphs that illustrate the extent of the bulging of the back surface of a target during complete penetration. The copper, aluminum, and steel targets investigated behave in a manner similar to that shown in these shadowgraphs when completely penetrated.

As can be seen, most of the target material forming the back-surface bulge spalls from the target as the projectile completes its penetration. The spalled particles have a velocity distribution varying from the exit velocity of the projectile for the first spalled pieces near the penetrated hole (3,000 ft/sec in this case) down to a velocity of only approximately 1,000 ft/sec for the larger pieces which spalled later. It is apparent from this photograph that if this plate were the protective covering for a missile, then the interior of the missile would not only be subject to damage from the penetrating particle but also to damage inflicted by these spalled particles. It should be added, however, that the relatively thin flat shapes of the greater number of the particles spalled from a target during penetration would prevent them from having much penetrating capability were they to strike objects in the interior of the vehicle. During this investigation it was

observed that the spalled particles were able to penetrate only slightly the surface of soft pine blocks placed 6 inches from the target back surface.

## CONCLUSIONS

It has been found that for the projectile-target material combinations and the velocity spectrum used in this investigation, the penetration is a function of the target thickness provided that the penetration is greater than 20 percent of the target thickness. Targets of a thickness such that the penetration amounts to less than 20 percent of the thickness may be regarded as quasi-infinite. In particular, it has been found that a projectile can completely penetrate a target whose thickness is approximately one and one-half times as great as the penetration of a similar projectile into a quasi-infinite target.

The diameter of a crater has also been found to be a function of the target thickness provided that the target thickness is not greater than the projectile length in the case of cylindrical projectiles and not greater than two to three times the projectile diameter in the case of spherical projectiles.

Langley Research Center,
National Aeronautics and Space Administration,
Langley Field, Va., August 28, 1958.

## REFERENCES

1. Charters, A. C., and Locke, G. S., Jr.: A Preliminary Investigation of High-Speed Impact: The Penetration of Small Spheres Into Thick Copper Targets. NACA RM A58B26, 1958.

2. Kinard, William H., and Lambert, C. H., Jr.: An Investigation of the Effect of Target Temperature on Projectile Penetration and Cratering. NACA RM L58E14, 1958.

3. Sewell, Robert G. S., Cosner, Lawrence N., Wedaa, Henry W., and Gallup, Rolland: High-Framing-Rate, Argon-Flash Field Photography. NAVORD Report 5298 (NOTS 1528), U. S. Naval Ord. Test Station (China Lake, Calif.), Oct. 9, 1956.

4. Romine, H. E.: Direct Contact Explosion Effect on Ordnance Materials - Tests on Mild Steel, STS Armor and 2024-T4 Aluminum Alloy Plates $1\frac{1}{2}$ Inches Thick. NPG Rep. No. 1535, U. S. Naval Proving Ground (Dahlgren, Va.), Apr. 29, 1957. (Available from ASTIA as AD No. 129298.)

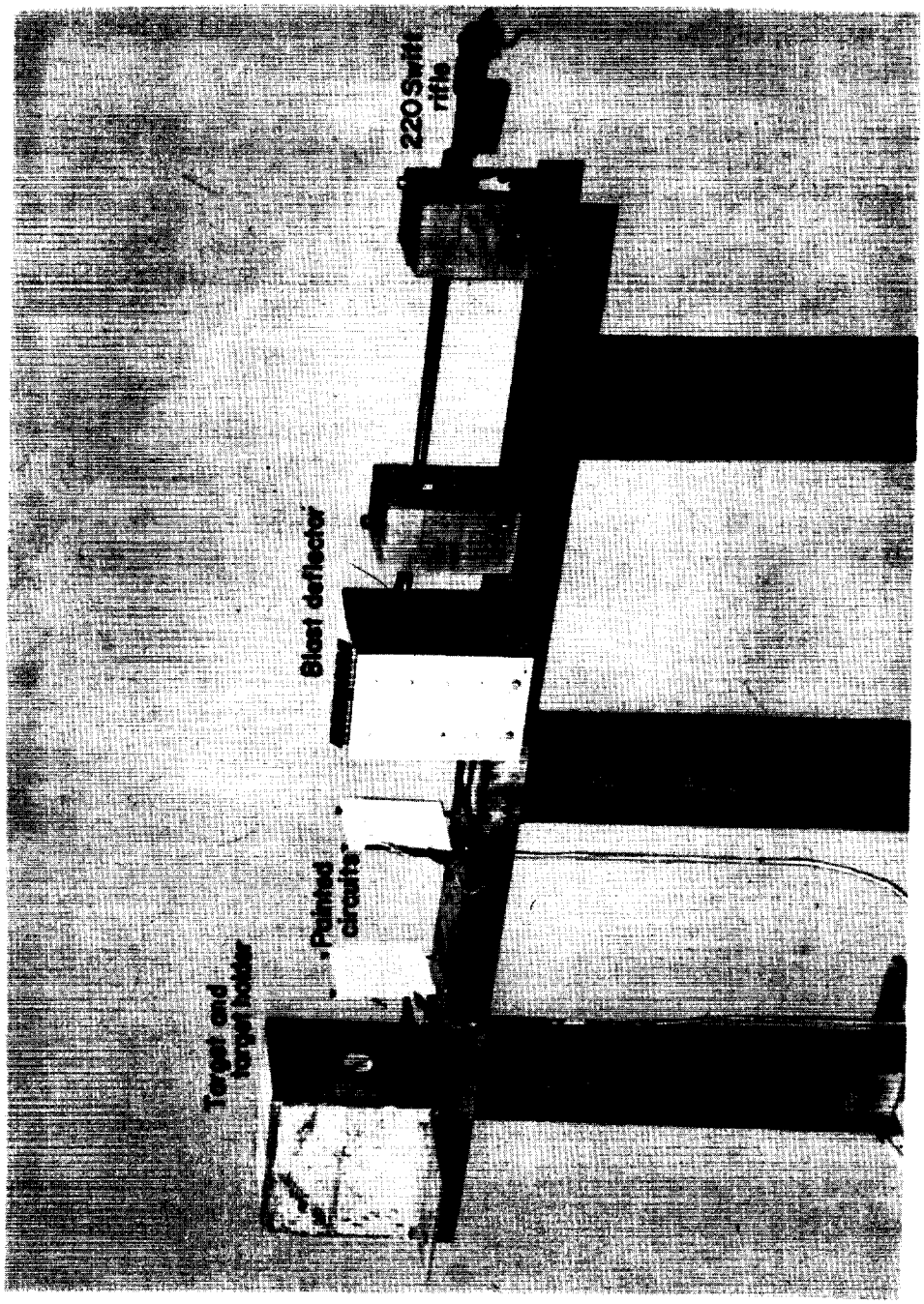


L-57-3298.1

Figure 1.- General arrangement of 220 Swift rifle used in making impact studies.

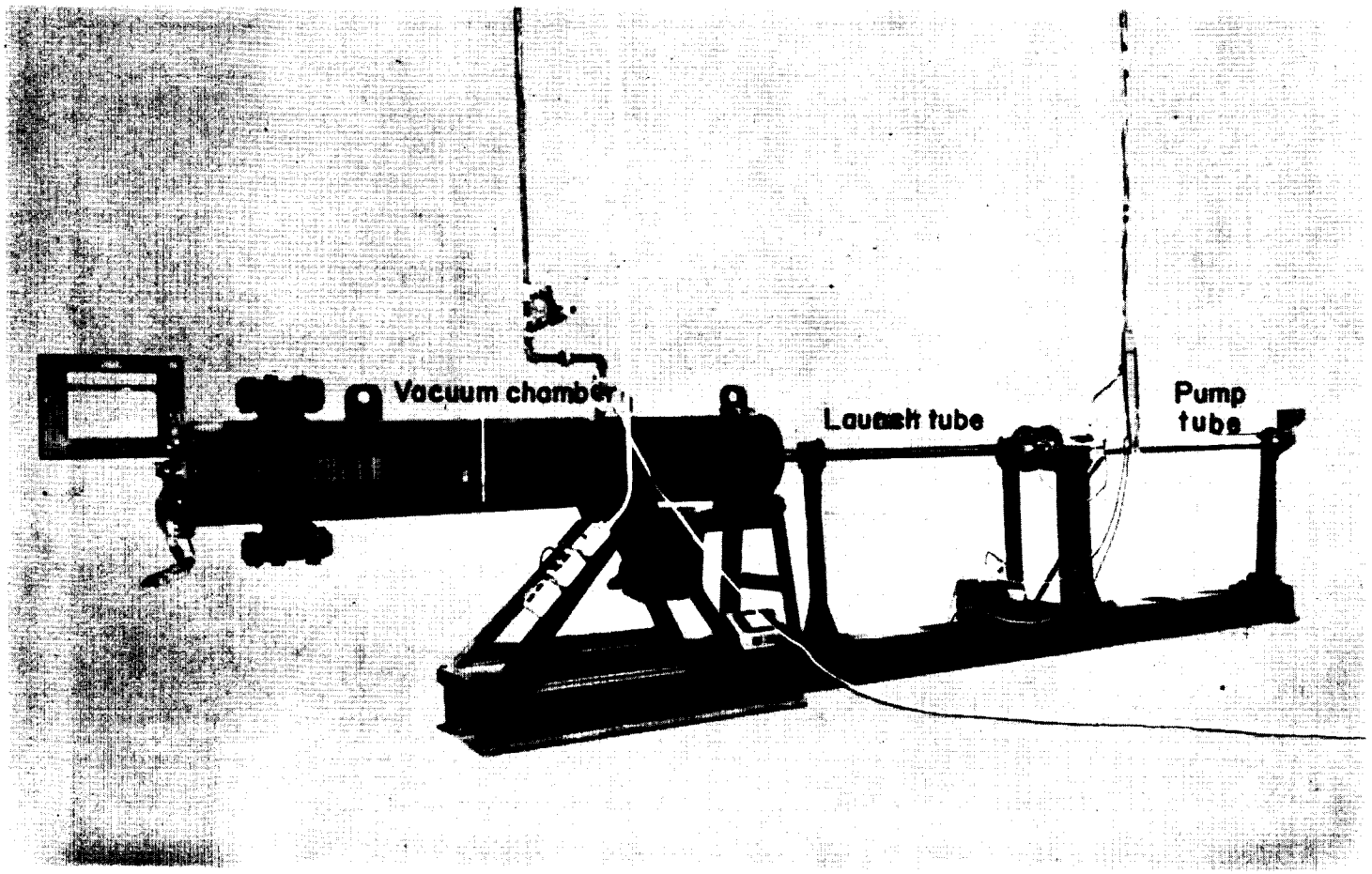


Figure 2.- Helium-gun installation. L-57-4364.1

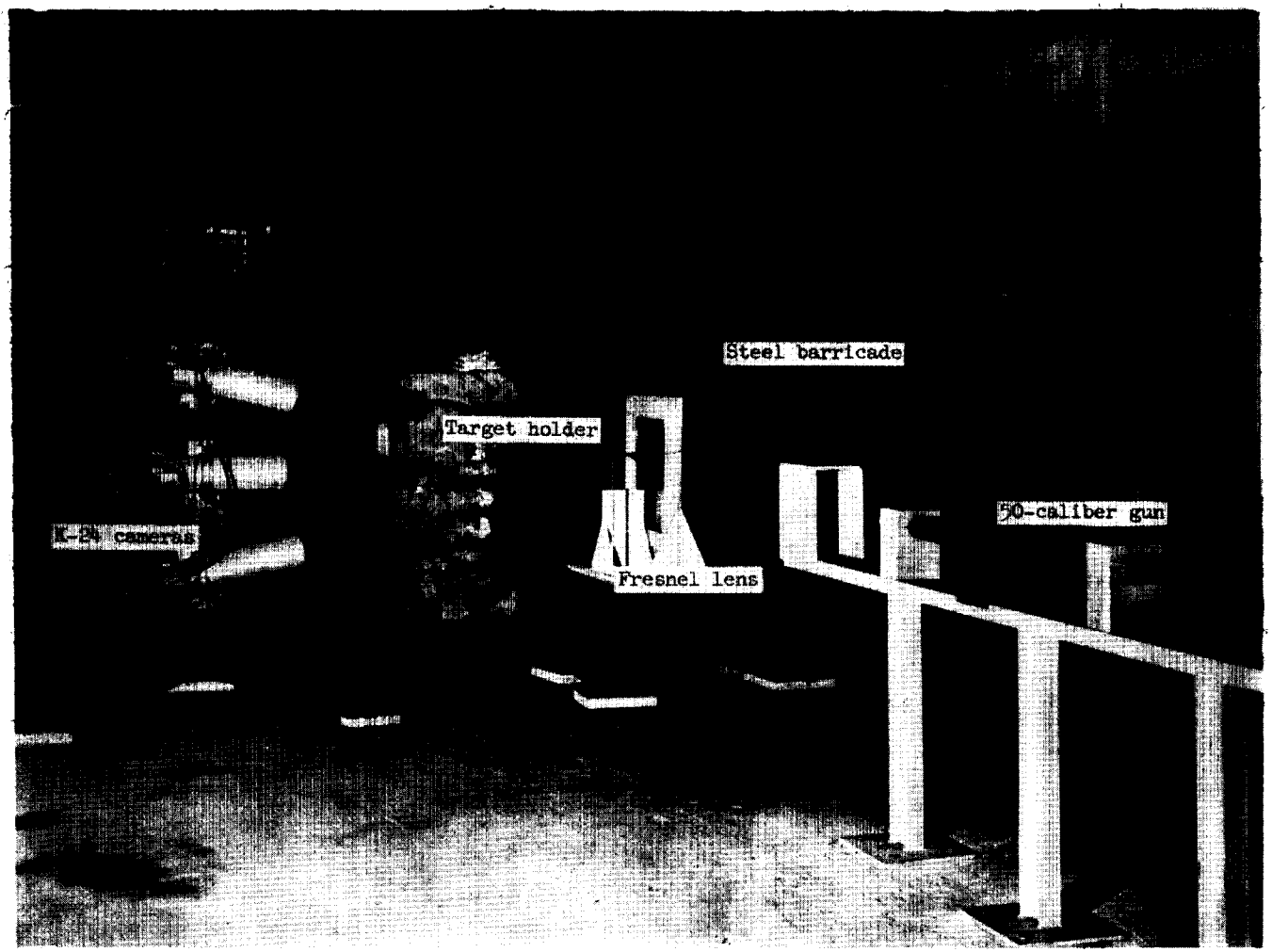


L-58-1878.1

**Figure** 3.- Arrangement of the 50-caliber gun and the high-framing-rate, argon-flash **photography** equipment.

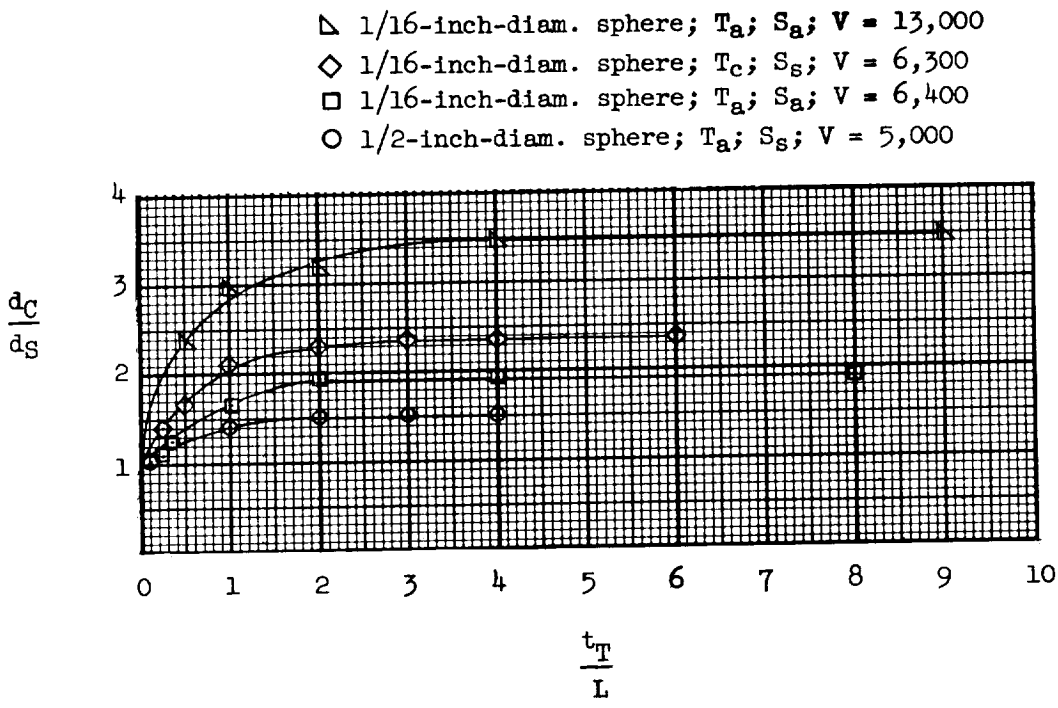


(a) Sphere impacts.

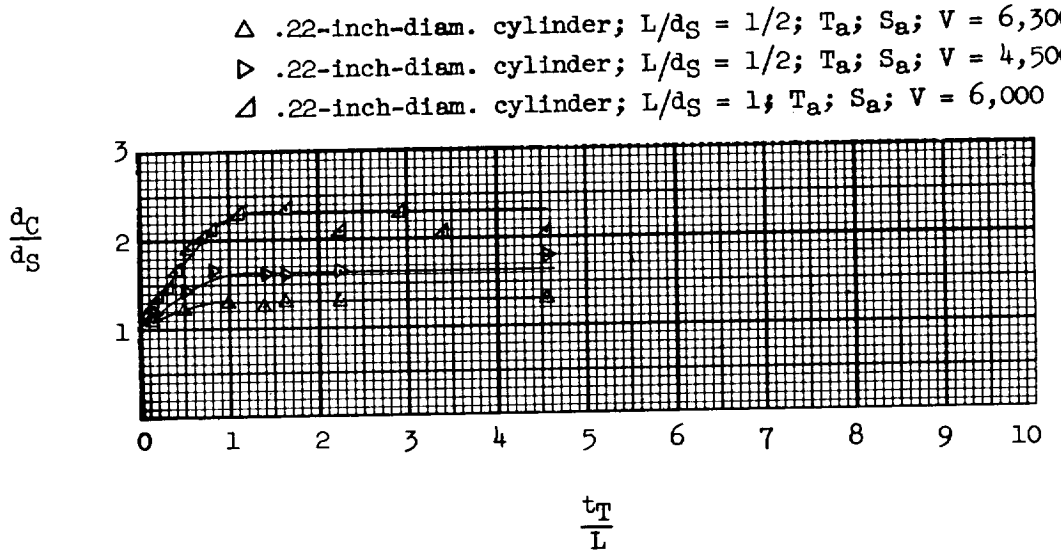


(b) Cylinder impact.

Figure 4.- Effect of target thickness on the diameter of craters formed by impacting projectiles.

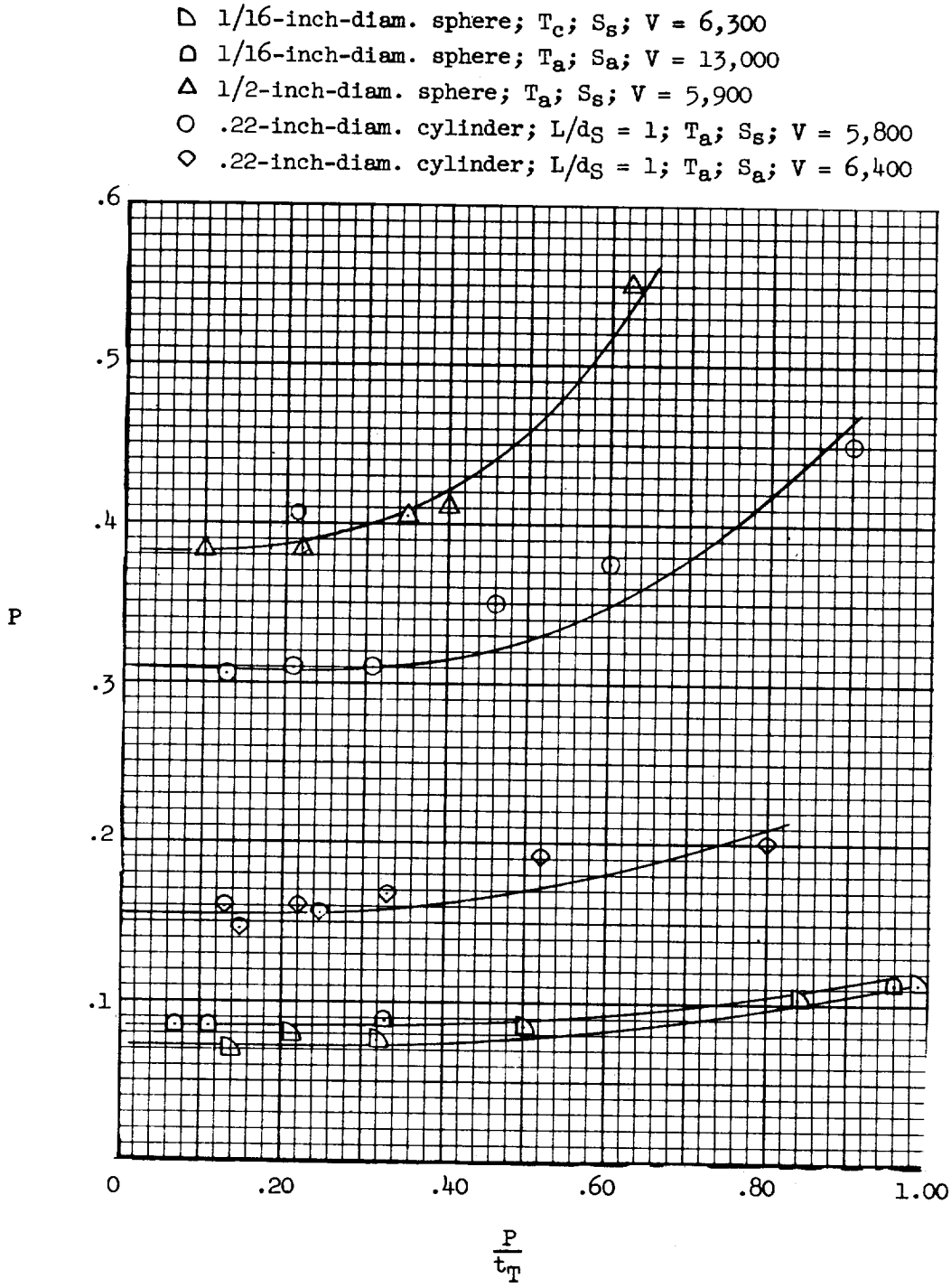


Figure 5.- Effect of target thickness on penetration of impacting projectiles.

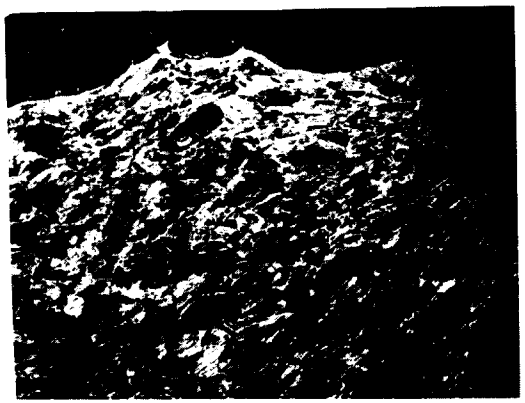

Section taken adjacent to crater bottom.

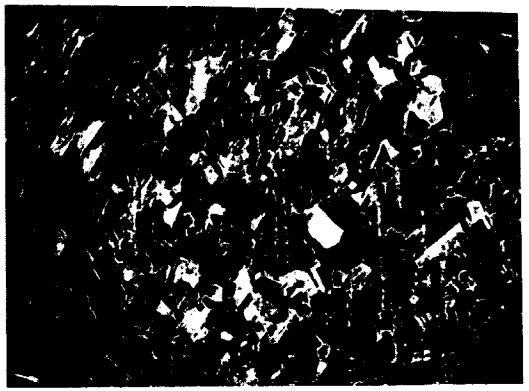

Section taken halfway between crater bottom and target back surface.

Section taken adjacent to target back surface.

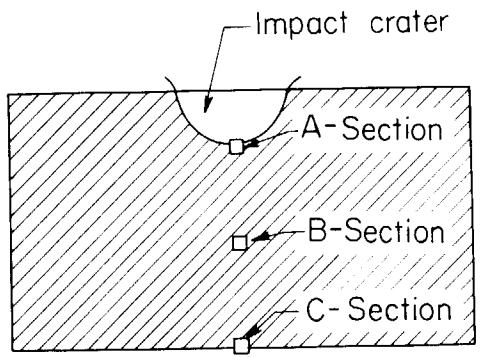


Schematic diagram showing location of photomicrographs with respect to target cross-section.

L-58-2538

Figure 6.- Photomicrographs showing grain structure in a copper target after being impacted. (0 to 30 percent nitric acid etch and a magnification factor of x120.)

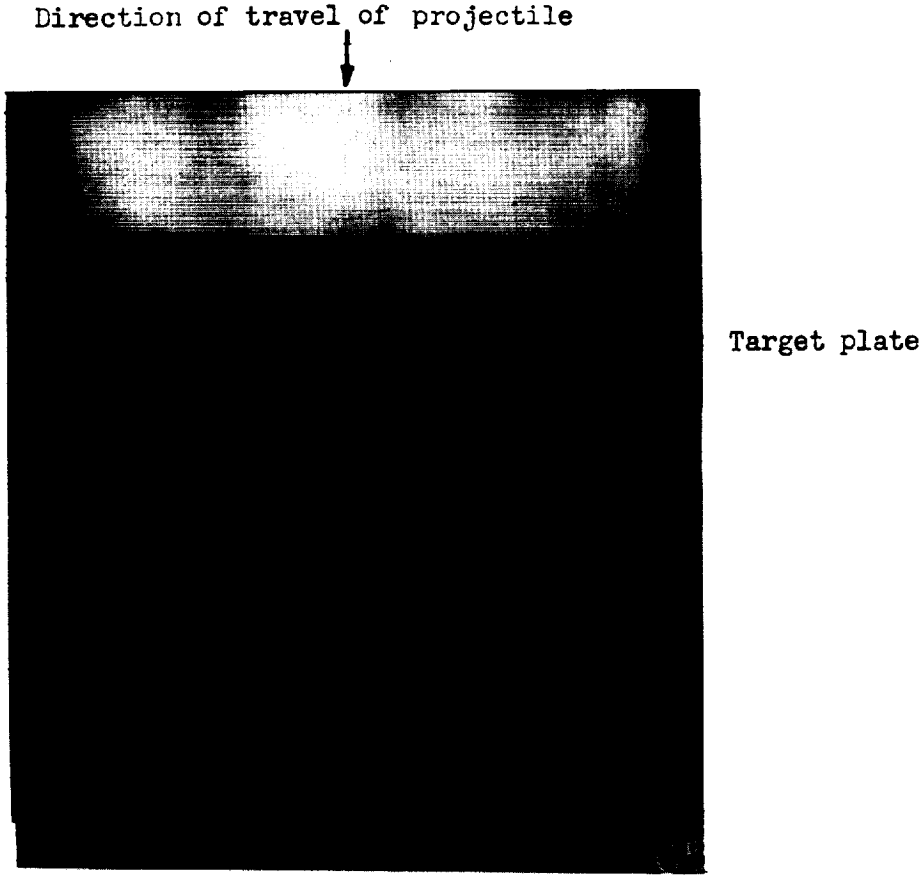


L-58-2539

Figure 7.- Shadowgraph showing the bulging of the back surface of a 1-inch aluminum plate being impacted by a $\frac{1}{2}$- inch-diameter sphere.

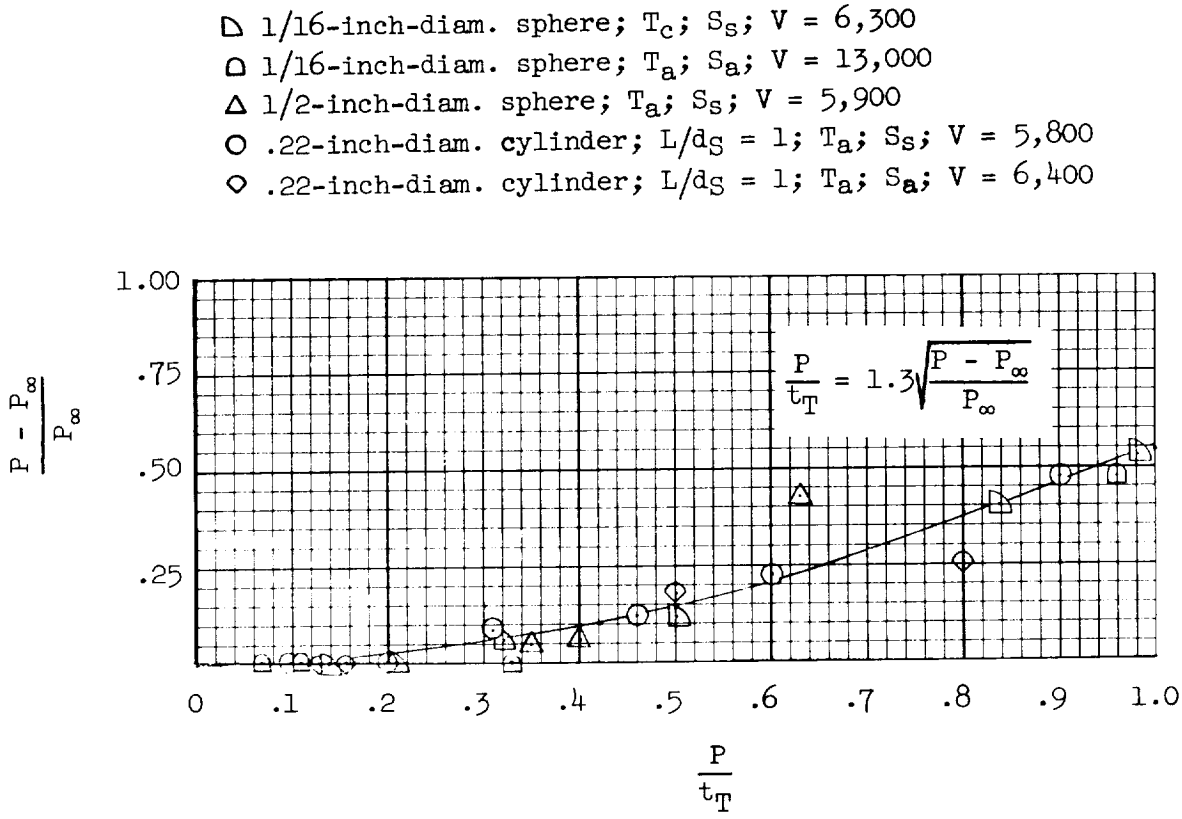


Figure 8.- Percent gain in penetration above that achieved in a quasi-infinite target plotted against the percent of the target thickness penetrated.

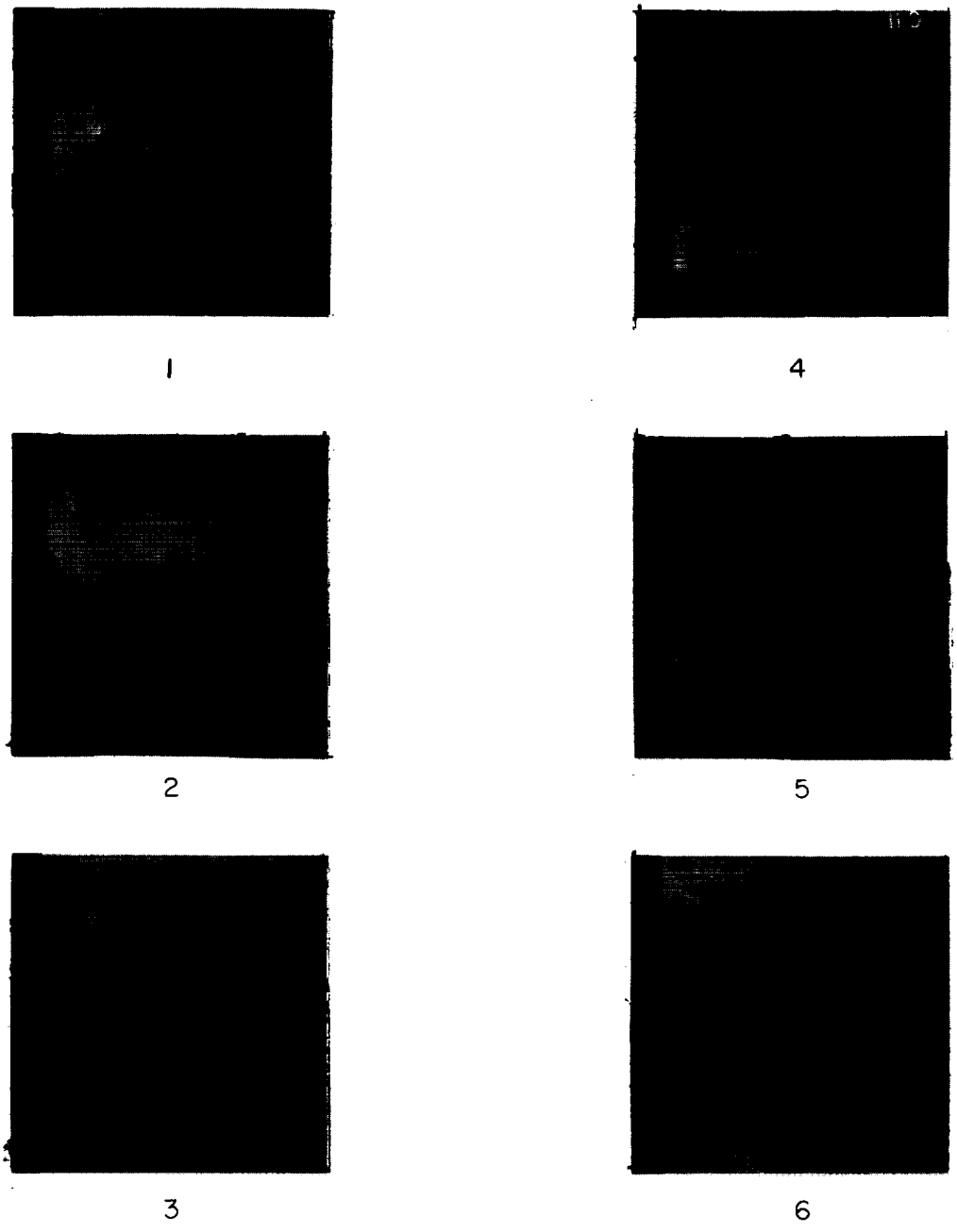


L-58-2537

Figure 9.- The $\frac{1}{2}$-inch-diameter steel ball completely penetrating 1-inch-thick aluminum target. Impact velocity, 5,100 ft/sec.

NASA - Langley Field, Va.

NASA MEMO 10-18-58L
National Aeronautics and Space Administration.
EFFECT OF TARGET THICKNESS ON CRATERING AND PENETRATION OF PROJECTILES IMPACTING AT VELOCITIES TO 13,000 FEET PER SECOND.
William H. Kinard, C. H. Lambert, Jr., David R. Schryer, and Francis W. Casey, Jr. December 1958. 20p. diagrs., photos.
(NASA MEMORANDUM 10-18-58L)
(Title, Unclassified)

It has been found that, for the projectile velocities and target and projectile materials considered, the depth of penetration of a target is a function of the target thickness provided that the penetration is greater than 20 percent of the target thickness. The diameter of a crater has also been found to be a function of the target thickness provided that the target thickness is not greater than the projectile length in the case of cylindrical projectiles, and not greater than two to three times the projectile diameter in the case of spherical projectiles.

Copies obtainable from NASA, Washington

1. Materials, Properties - Plasticity (5. 2. 13)
2. Research Equipment, Materials (9. 1. 6)
3. Research Technique (9. 2)

I. Kinard, William H.
II. Lambert, C. H., Jr.
III. Schryer, David R.
IV. Casey, Francis W., Jr.
V. NASA MEMO 10-18-58L

NASA

NASA MEMO 10-18-58L
National Aeronautics and Space Administration.
EFFECT OF TARGET THICKNESS ON CRATERING AND PENETRATION OF PROJECTILES IMPACTING AT VELOCITIES TO 13,000 FEET PER SECOND.
William H. Kinard, C. H. Lambert, Jr., David R. Schryer, and Francis W. Casey, Jr. December 1958. 20p. diagrs., photos.
(NASA MEMORANDUM 10-18-58L)
(Title, Unclassified)

It has been found that, for the projectile velocities and target and projectile materials considered, the depth of penetration of a target is a function of the target thickness provided that the penetration is greater than 20 percent of the target thickness. The diameter of a crater has also been found to be a function of the target thickness provided that the target thickness is not greater than the projectile length in the case of cylindrical projectiles, and not greater than two to three times the projectile diameter in the case of spherical projectiles.

Copies obtainable from NASA, Washington

1. Materials, Properties - Plasticity (5. 2. 13)
2. Research Equipment, Materials (9. 1. 6)
3. Research Technique (9. 2)

I. Kinard, William H.
II. Lambert, C. H., Jr.
III. Schryer, David R.
IV. Casey, Francis W., Jr.
V. NASA MEMO 10-18-58L

NASA

NASA MEMO 10-18-58L
National Aeronautics and Space Administration.
EFFECT OF TARGET THICKNESS ON CRATERING AND PENETRATION OF PROJECTILES IMPACTING AT VELOCITIES TO 13,000 FEET PER SECOND.
William H. Kinard, C. H. Lambert, Jr., David R. Schryer, and Francis W. Casey, Jr. December 1958. 20p. diagrs., photos.
(NASA MEMORANDUM 10-18-58L)
(Title, Unclassified)

It has been found that, for the projectile velocities and target and projectile materials considered, the depth of penetration of a target is a function of the target thickness provided that the penetration is greater than 20 percent of the target thickness. The diameter of a crater has also been found to be a function of the target thickness provided that the target thickness is not greater than the projectile length in the case of cylindrical projectiles, and not greater than two to three times the projectile diameter in the case of spherical projectiles.

Copies obtainable from NASA, Washington

1. Materials, Properties - Plasticity (5. 2. 13)
2. Research Equipment, Materials (9. 1. 6)
3. Research Technique (9. 2)

I. Kinard, William H.
II. Lambert, C. H., Jr.
III. Schryer, David R.
IV. Casey, Francis W., Jr.
V. NASA MEMO 10-18-58L

NASA

NASA MEMO 10-18-58L
National Aeronautics and Space Administration.
EFFECT OF TARGET THICKNESS ON CRATERING AND PENETRATION OF PROJECTILES IMPACTING AT VELOCITIES TO 13,000 FEET PER SECOND.
William H. Kinard, C. H. Lambert, Jr., David R. Schryer, and Francis W. Casey, Jr. December 1958. 20p. diagrs., photos.
(NASA MEMORANDUM 10-18-58L)
(Title, Unclassified)

It has been found that, for the projectile velocities and target and projectile materials considered, the depth of penetration of a target is a function of the target thickness provided that the penetration is greater than 20 percent of the target thickness. The diameter of a crater has also been found to be a function of the target thickness provided that the target thickness is not greater than the projectile length in the case of cylindrical projectiles, and not greater than two to three times the projectile diameter in the case of spherical projectiles.

Copies obtainable from NASA, Washington

1. Materials, Properties - Plasticity (5. 2. 13)
2. Research Equipment, Materials (9. 1. 6)
3. Research Technique (9. 2)

I. Kinard, William H.
II. Lambert, C. H., Jr.
III. Schryer, David R.
IV. Casey, Francis W., Jr.
V. NASA MEMO 10-18-58L

NASA